

## Article

# Plant Triterpenoids Regulate Endophyte Community to Promote Medicinal Plant *Schisandra sphenanthera* Growth and Metabolites Accumulation

Chuan You <sup>1,†</sup>, Dan Qin <sup>1,2,†</sup>, Yumeng Wang <sup>1</sup>, Wenyi Lan <sup>1</sup>, Yehong Li <sup>1</sup>, Baohong Yu <sup>1</sup>, Yajun Peng <sup>1</sup>, Jieru Xu <sup>1</sup> and Jinyan Dong <sup>1,\*</sup>

- <sup>1</sup> Chongqing Key Laboratory of Plant Resource Conservation and Germplasm Innovation, School of Life Sciences, Southwest University, Chongqing 400715, China; youchuan@email.swu.edu.cn (C.Y.); qindan2017@email.swu.edu.cn (D.Q.); w928986123@email.swu.edu.cn (Y.W.); lanlalawy@email.swu.edu.cn (W.L.); 18008338842@email.swu.edu.cn (Y.L.); ba323575@email.swu.edu.cn (B.Y.); peng199595@email.swu.edu.cn (Y.P.); xjr960313@email.swu.edu.cn (J.X.)
- <sup>2</sup> Key Scientific Research Base of Pest and Mold Control of Heritage Collection (Chongqing China Three Gorges Museum), State Administration of Cultural Heritage, Chongqing 400015, China
- \* Correspondence: donjyaa@swu.edu.cn
- † These authors contributed equally to this work and should be considered co-first authors.

**Abstract:** Beneficial interactions between endophytes and plants are critical for plant growth and metabolite accumulation. Nevertheless, the secondary metabolites controlling the feedback between the host plant and the endophytic microbial community remain elusive in medicinal plants. In this report, we demonstrate that plant-derived triterpenoids predominantly promote the growth of endophytic bacteria and fungi, which in turn promote host plant growth and secondary metabolite productions. From culturable bacterial and fungal microbial strains isolated from the medicinal plant *Schisandra sphenanthera*, through triterpenoid-mediated screens, we constructed six synthetic communities (SynComs). By using a binary interaction method in plates, we revealed that triterpenoid-promoted bacterial and fungal strains (TPB and TPF) played more positive roles in the microbial community. The functional screening of representative strains suggested that TPB and TPF provide more beneficial abilities to the host. Moreover, pot experiments in a sterilized system further demonstrated that TPB and TPF play important roles in host growth and metabolite accumulation. In summary, these experiments revealed a role of triterpenoids in endophytic microbiome assembly and indicated a strategy for constructing SynComs on the basis of the screening of secondary metabolites, in which bacteria and fungi join forces to promote plant health. These findings may open new avenues towards the breeding of high yielding and high metabolite-accumulating medicinal plants by exploiting their interaction with beneficial endophytes.

**Keywords:** endophyte; triterpenoid; *Schisandra sphenanthera*; SynCom; interactions; growth; metabolites



**Citation:** You, C.; Qin, D.; Wang, Y.; Lan, W.; Li, Y.; Yu, B.; Peng, Y.; Xu, J.; Dong, J. Plant Triterpenoids Regulate Endophyte Community to Promote Medicinal Plant *Schisandra sphenanthera* Growth and Metabolites Accumulation. *J. Fungi* **2021**, *7*, 788. <https://doi.org/10.3390/jof7100788>

Academic Editor: Gary A. Strobel

Received: 12 September 2021

Accepted: 16 September 2021

Published: 23 September 2021

**Publisher's Note:** MDPI stays neutral with regard to jurisdictional claims in published maps and institutional affiliations.



**Copyright:** © 2021 by the authors. Licensee MDPI, Basel, Switzerland. This article is an open access article distributed under the terms and conditions of the Creative Commons Attribution (CC BY) license (<https://creativecommons.org/licenses/by/4.0/>).

## 1. Introduction

Endophytes (fungi and bacteria) colonize the tissue or intercellular spaces of various plant organs, live in healthy plants, at least at a certain stage or even during the whole life cycle, and do not cause obvious plant diseases [1]. The endophytic microbiome plays an important role in different functions such as plant growth, development, signal network, gene expression, metabolic pathways and response to biological stress [2–4]. The microbial community compositions of root, stem and leaf were clearly distinguished from rhizosphere soil and nonrhizosphere [5]. Plants actively recruit and nurture a collection of microbes from the soil to live in the vicinity, on the surface and inside their tissues [1]. Endophytic microbes provide various essential nutrients (i.e., nitrogen and phosphorous) to the host species, which promote plant growth and increase environmental tolerance and phytopathogenic resistance. In return, the plant partners offer stable niches and photosynthetic productions

to the endophytes [6]. However, few studies have reported on the secondary metabolites that influence the assemblies of the endophytic microbiome in plants.

Plants have evolved their special secondary metabolites for metabolism, growth, development, and resistance to drought, disease, and radiation in natural environments [7]. An increasing body of evidence highlights the strong influences of secondary metabolites on the assembly and function of the plant microbiome. A group of secondary metabolites is involved in shaping the plant microbiome in the plant kingdom, such as triterpene [8], coumarin [9], camalexin [10], glucosinolate [2], and benzoxazinoid [11]. Plant secondary metabolites can exert a wide spectrum of effects upon individual microbial strains by functioning as signaling molecules, nutrient sources, or toxins [12]. In return, microbes promote host plant growth and health through enhancement of nutrient uptake, inhibition of pathogens, and maintenance of community stability [9,13,14]. Triterpenoid derivatives have functions in plant defense, signaling, and antimicrobial activity. Recent studies demonstrated that triterpenoids can selectively regulate the growth of *Arabidopsis thaliana* root bacteria from different taxa [8]. With respect to the microbiome, endophytes affect plant growth and development by enhancing nutrient uptake, producing indole acetic acid, and alleviating stresses [14]. Endophytic microbial strains form a stable community structure through cooperation and competition to survive in and colonize plants [15–19]. For example, previous studies on *A. thaliana*, soybean, tomato, garlic, and *Salvia miltiorrhiza* demonstrated that microbial interactions play an essential role in plant growth, health, and metabolite accumulation through some mechanisms including increasing antibiotic secretion, promoting biofilm formation and growth, and influencing metabolic pathways [14,20–25].

There are about 58 species in the world, which are mainly distributed in Southeast Asia and North America, and 29 species in China of the Schisandraceae family. As a widely domesticated medicinal plant in China, the Schisandraceae family has a very important position in China's traditional medicine [26]. Furthermore, numerous secondary metabolites with wide biological activity were isolated from Schisandraceae plants, among which lignans and triterpenoids are the predominant groups. Since 1970, more than 1000 terpenotypes of schtriterpenoids/schnortriterpenoids have been reported to be produced by the plants of Schisandraceae family [27]. Our previous studies demonstrated that endophytic fungi can specifically utilize and transform host triterpenoids in vitro [28,29]. Thus, triterpenoids may play a role in shaping the endophytic microbiome in the plant.

In this study, we collected a Schisandraceae plant species from a natural environment in Xichou county of Yunnan province, corresponding to *S. sphenanthera*, and isolated and identified the culturable bacterial and fungal strains across 20 samples from multiple organs (root, stem, leaf, and fruit) of the plant species. Through in vitro bioassays with purified compounds of triterpenoids, the selective growth modulation activities of triterpenoids toward endophytes in *S. sphenanthera* were identified. The functional screening of culturable strains proved that triterpenoid-promoted bacterial and fungal strains (TPB and TPF) are beneficial microbes of plants. Then, we investigated the interaction between representative bacteria and endophytic fungi in vitro. Germ-free *S. sphenanthera* were further established to elucidate the activities of the synthetic communities (SynComs) with the greatest effect on *S. sphenanthera* growth and metabolic accumulation.

## 2. Materials and Methods

### 2.1. Sampling of *S. Sphenanthera* Plants in the Natural Habitat

Healthy *S. sphenanthera* were collected in June of 2019 at Xichou, Yunnan province, China (altitude: 1399 m, 23°38.114', E104°79.155'). Samples were taken from five *S. sphenanthera* plants separated by a variable distance ranging from 1 to 10 m. The plants were chosen without regard to their age or size. Five individual plants were dug out, transported on ice to the laboratory, and stored at −80 °C. Sample fractionation into fruits, leaves, stems, and roots was performed within 12 hours after harvesting. Lastly, 500 segments from each plant organ were plotted for the isolation of endophytic bacteria and fungi.

## 2.2. Isolation, Purification, Identification, and Preservation of Culturable Bacteria and Fungi

In order to isolate endophytic fungi and bacteria, the plants were surface sterilized for 3 min in 80% EtOH, followed by a second sterilization step for 3 min in 0.25% NaClO. After washing the plants five times with sterile water, the fruits, leaves, roots, and stems were cut into small pieces (about  $2 \times 2$  mm) and placed onto PDA, M + PDA, and CMM media (Table S1) [30]. Endophytic fungi were purified and isolated by the tip mycelium picking method. Similarly, endophytic bacteria were isolated from plants on TSB, TYG, YEM, TWYE, MYX, MM+MeOH, R2A, MMF, and GAM, and purified by dilution (Table S1) [31]. The DNA of the purified strains was extracted and amplified by PCR using bacterium-specific primers (1494R, 27F) and fungus-specific primers (ITS1, ITS4). The products were purified and sequenced in two directions. The 16S rRNA or ITS rRNA sequences were obtained by splicing the upstream and downstream sequences. Blast comparison was carried out in the NCBI GenBank database to find representative sequences that had a greater than 97% similarity. In total, 127 bacterial isolates and 119 fungal isolates were successfully identified according to their morphology and their 16S rDNA and ITS rDNA sequences, respectively. Further phylogenetic tree analysis of sequenced isolates was conducted with multiple sequence alignments constructed in Clustal W [32] using the neighbor-joining method in MEGA 7.0 and visualized with iTOL v4 [33]. All collected isolates from plants were subsequently frozen in 30% or 40% glycerol stock solutions at  $-80$  °C for storage.

## 2.3. Isolation of Main Triterpenoid Metabolites from *S. sphenanthera*

Samples of roots, stems, leaves, and fruits (10 kg) from five *S. sphenanthera* plants were cut into pieces and dried naturally. After drying, the plant organs were soaked in 20 L of acetone for 15 days. The extraction was repeated a total of five times to fully extract the metabolites in the plant. The acetone extract was evaporated under reduced pressure in a rotary evaporator to obtain the crude extract. After extraction, the crude extract was subjected to MCI (CHP20P, 75~150  $\mu$ ; Mitsubishi Chemical Corporation) column chromatography (CC) eluted with a gradient of CH<sub>3</sub>OH–H<sub>2</sub>O (1:9–1:0, 25 mL/min, 12 h) to afford 10 fractions (Fr. A–J) based on the basis of TLC pattern. Fraction C was purified over silica gel (chloroform–EtOAc, 10:1) and Sephadex LH-20 (MeOH) to furnish compound S4 (2.1 g). Fraction E (6 g) was further purified by silica gel column chromatography and eluted with gradient mixtures of petroleum ether EtOAc and AcOH (6:4:0.1) to yield compound S1 (9.0 g) and S2 (3.6 g). Fraction K was subjected to Sephadex LH-20 column eluted with MeOH and recrystallized to obtain compound S3 (4.5 g). The purity of all the isolated triterpenoids was greater than 95%, and the purity of all isolated triterpenoids was determined by HPLC analysis, which was carried out using an Agilent L-2000 liquid chromatograph equipped with a Zorbax SB-C18 (Agilent Technologies, Santa Clara, California, 9.4 mm  $\times$  15 cm column), The detection wavelengths of compounds S1–S4 were 212 nm (LC-UV%), 217 nm (LC-UV%), 203 nm (LC-UV%) and 243 nm (LC-UV%).

## 2.4. In Vitro Assay for Selective Effect of Triterpenoids

In total, 27 bacterial isolates and 26 fungal isolates from diverse taxa were selected for bioassay. To quantify the effect of triterpenoids on growth of the endophytic bacteria in vitro, we designed a microplate assay with a 96-well flat-bottomed plate on the basis of Huang et al. and Stringlis et al. [8,9]. Each assayed compound (compounds S1–S4) was mixed at a ratio of 1:1 in weight, and then was dissolved with ethanol to prepare a mix solution with different concentrations. Solvent ethanol was used as a control. A single colony from each strain was picked and inoculated into a 1/2TSB broth (Tryptone, Soya Broth (Oxoid) 15 g/L) and cultured at 37 °C overnight until the density reached OD<sub>600</sub> 0.5–1.0. The cultures were then diluted 20–40 fold with 1/10TSB medium depending on the growth rate of the individual bacterial strain, and the resulting broth was used for bioassay. The growth medium was supplemented with different concentrations of triterpenoid mixtures and EtOH only in 1/2TSB media, and growth (OD<sub>600</sub>) was monitored over 72 h

in the dark at 37 °C. The selective effect of endophytic fungus growth by triterpenoids *in vitro* was tested in a 6-well flat-bottomed plate by subculturing a mycelium plug of 5 mm diameter on 1/5 liquid potato dextrose broth (PDB) containing different concentrations of triterpenoid mixtures for 12 days in the dark at 28 °C. The mycelium was centrifuged at 12,000 g to remove the medium, and growth was recorded by weighing the fresh mycelium weight at 12 days.

### 2.5. Functional Screening for Potentially Beneficial Microbes

The procedure was used to screen for potentially beneficial microbes from 170 bacterial isolates and 170 fungal isolates. Bacterial and fungal indole 3-acetic acid (IAA) production was measured by using Salkowski reagent, as described by Hussain et al. [34]. The 500 µL of bacterial and fungal inoculum was dispensed in 100 mL TSB or PDA broth alone, or supplemented with 1% tryptophan, respectively. Bacterial and fungal strains were grown in broth for 24 h and 7 days, respectively, at 28 °C. A 1 mL bacterial or fungal supernatant was mixed with 2 mL of Salkowski reagent (4.5 g of FeCl<sub>3</sub> per liter in 10.8 M H<sub>2</sub>SO<sub>4</sub>) and incubated at room temperature for 30 min. The developed color was monitored at 535 nm by using a CECIL Aquarius CE 7200 spectrophotometer (UK).

To evaluate siderophore production, CAS medium (blue agar chrome azurol S (CAS), medium containing chrome azurol S (CAS), and hexadecyltrim ethylammonium bromide (HDTMA)) were used to determine the siderophore production of the selected strains, as described by Alexander et al. [35]. Then, 500 µL of bacterial and fungal inoculum was dispensed in 100 mL TSB or PDA broth containing no added Fe, respectively. Bacterial and fungal strains were grown for 24 h and 7 days, respectively, at 28 °C. Siderophore concentration in the bacterial or fungal supernatant was measured by mixing 100 µL of modified CAS assay solution with 100 µL supernatant in a 96-well plate. Absorbance was measured at 630 nm with a microplate reader.

For the determination of the 1,1-diphenyl-2-picrylhydrazyl (DPPH) radical, 100 µL of an aqueous solution of the bacterial and fungal supernatant sample (control:100 µL of distilled water) was added to an ethanolic solution of DPPH (60 µM) in microwells, according to the method of Yokozawa et al. [36]. After incubation, the DPPH radical was determined using a microplate reader.

For P-solubilizing activity assays, P content in the fermentation liquid of bacteria and fungi was established by Mo-Sb colorimetry, as described by Gyaneshwar et al. [37]. Then, 1 mL of an aqueous solution of the bacterial and fungal supernatant sample (control:1 mL of phosphate solution) was added to 1% ascorbic acid solution (1 mL), followed by 2 mL of molybdate solution added after 30 s and reacted for 10 min. Lastly, absorbance was measured at 720 nm with a microplate reader.

### 2.6. Assessment of Dual Interactions in Culture Media

Dual interactions of the 27 bacterial species were tested in the solid TSB agar (Figure S6a) [20]. A single colony from each strain was picked and then inoculated into a 1/2TSB broth and incubated overnight at 37 °C at 180 rpm. The optical density of bacterial cultures was adjusted to 0.1 at 600 nm. Eleven times 1 µL of these dilutions were inoculated in a diagonal row on both sides of a circular culture dish with TSB agar with a multichannel pipet, creating a V shape of increasingly close inoculation sites. The plates were sealed with Parafilm and incubated for 15 days at 20 °C. Colony diameters were measured on a line, orthogonal to the line dividing the V shape. The interaction index (II) was calculated as follows:  $II = [(D_{25mm-EA}/D_{10mm-EA})/(D_{25mm-CA}/D_{10mm-CA}) - 1] * 100\%$  (with  $D_{25mm}$  and  $D_{10mm}$  representing the neighboring colony diameter at 25 and 10 mm horizontal distance to the V shape, respectively; and  $D_{EA}$  and  $D_{CA}$  being the bacterial strain on the V-shape of the experiment and control group, respectively). Dual interactions of 25 fungal species were tested in solid PDA agar (Figure S6b) [38]. Two mycelial disks with a diameter of 5 mm were placed in the center of a PDA plate with a distance of 2 cm. After growth at 28 °C for 3 days, scans were performed using a

Konica Minolta Bizhub C652 (Konica Minolta Business Solutions U.S.A., Inc., Ramsey, NJ, USA) and saved as JPEG images (3024 × 4032 px, file size ranged from 1.19 to 3.01 MB). Scans were analyzed using the National Institutes of Health Image J v1.4 measuring tool software ([rsb.info.nih.gov/ij/index.html](https://rsb.info.nih.gov/ij/index.html)). II was calculated as follows:  $II = (S_{EA}/S_{CA} - 1) * 100\%$  (where  $S_{EA}$  and  $S_{CA}$  represent the measured colony area of fungi on the plate of the experiment and control groups, respectively). Dual interactions of the 27 bacterial species and 25 fungal species were tested in the solid PDA agar (Figure S6c) [39]. A mycelial disk with a diameter of 5 mm was placed at 2 cm from the edge of a PDA plate. The 27-species bacterial suspension was streaked across the middle of the plate. A control was set up for challenging fungi without bacteria. After growth at 28 °C for 12 days, the diameter of the fungus colonies was recorded. II was calculated as follows:  $II = (S_{EA}/S_{CA} - 1) * 100\%$  (where  $S_{EA}$  and  $S_{CA}$  represented the colony diameter of fungi in the experiment and control group, respectively). II values below or above zero indicated growth inhibition and facilitation, respectively, and they were expressed as percentage fold changes.

### 2.7. SynCom Construction and Functional Evaluation

Surface-sterilized seeds of *S. sphenanthera* with 95% alcohol and sodium hypochlorite were planted in the sterilized soil and cultured at 28 °C for 90 days (see Figure S11C). The young stem segments were cut for the rapid clonal propagation of *S. sphenanthera*. The propagation medium was MS + BA (1.0 mg/L) + NAA (0.03 mg/L), and the rooting medium was 1/2MS + IBA (0.5 mg/L). After the aseptic seedlings of *S. sphenanthera* had taken root (see Figure S11A,B), the plants with the same growth momentum were transplanted into the sterilized soil in a culture bottle (see Figure S11C) [40]. Tissue cultures of *S. sphenanthera* were planted in a small bottle with sterilized soil, on the basis of Liu et al. [25]. Three plants were sown in each pot, and three pots were set up for each treatment. For the construction of the synthetic community (SynCom), a total of 52 isolates were selected from diverse taxa [14]. The strain composition of the six SynComs was based on Tables S1 and S2. Bacterial strains were cultivated in 400 mL of 1/2 TSB overnight at 37 °C. These bacteria were centrifuged at 3000 × *g* for 10 min and resuspended in 10 mM MgCl<sub>2</sub> solution. Prior to inoculation, OD<sub>600</sub> of the bacterial solution was diluted to 0.02 (107 cells/mL). Fungal strains were cultivated in 400 mL of PDB at 28 °C for 10 days. The mycelium pieces were collected and dispersed in 10 mM MgCl<sub>2</sub> solution containing stainless-steel beads (3 mm). Then, 5 g of mycelium was dissolved in 50 mL 1/2 MS medium for co-culture system inoculation. After that, 1 mL of bacteria and 50 mL of fungi were inoculated by syringe into the root-soil of three-week-old *S. sphenanthera* seedlings with the same growth conditions [41]. SynCom inoculants were prepared through mixing equal amounts of each re-suspended microbial strain. All plants were grown in growth chambers for 60 days under long-day conditions (day/night: 14/10 h, 26/22 °C; light intensity: 2000 LX). Control plants were only supplied with 1/2 MS [4]. After 40 days, the plants were taken out and washed to measure their growth and physiological indices, including plant height, biomass, and chlorophyll content, and the content of metabolites. The whole plants of *S. sphenanthera* were dried in an oven at 55 °C for 24 h, and the dry weight of the plants was measured as biomass. To measure chlorophyll content, 200 mg of fresh leaf was extracted overnight in 8 mL of 80% (*v/v*) acetone, and absorbance at 645 and 663 nm was measured [42].

### 2.8. SEM Studies

To confirm the infection of bacteria and fungi in plants, scanning electron microscopy (JSM5910, JEOL, Japan) was used. The main roots of *S. sphenanthera* in the CK, AB, AF, and ABF group were collected after 28 days of co-culture, disinfected with 95% alcohol for 1 min, and fixed in 2.5% (*v/v*) glutaraldehyde (in 0.1M phosphate buffer; pH7.4) for 12 h at 4 °C. The roots were washed three times with 0.1M phosphate buffer for 5 min and dehydrated in a graded ethanol series (30%, 50%, 70%, 80%, 90%, 95%, and 100%) for 30 min each. Then, the root of *S. sphenanthera* was broken with a sterile scalpel, and the

sample was dried overnight in a sterile dryer. The total dried samples were then coated with gold ion and submitted for SEM analysis [43].

### 2.9. Measurement of Plant Metabolite Content

Total sugars, total triterpenoid, flavonoids, and polyphenols were determined to measure changes in plant metabolites. For determining total sugar content, 1 g of plant dried powder was ground with 50 mL water, then transferred into a centrifuge tube and centrifuged at  $5000\times g$  for 20 min at 4 °C. Then, the crude extract of total sugar was obtained through rotation–evaporation. The standard curve was analyzed with anhydrous glucose as the standard, and the content of total sugar in the crude extract was determined by classical phenol sulfuric acid spectrophotometry [44].

Total triterpenoid was measured on the basis of Sun et al. [45], using vanillin–acetic acid–perchloric acid spectrophotometry to detect total triterpenoid in plants. For determining total triterpenoid content, 1 g of plant dried powder was ground with 50 mL acetone, then transferred into a centrifuge tube and centrifuged at  $5000\times g$  for 20 min at 4 °C. Then, the crude extract of total triterpenoid was obtained through rotation–evaporation. Of pure petroleum ether, 20 mL was added to the crude extract to remove the chlorophyll from the solvent crude extract and centrifuged at  $5000\times g$  for 20 min at 4 °C. Then, 100 mL of isopropanol was added to dissolve the crude extract to be tested. Prepared ethanol standard solutions with different concentration gradients of nigranoic acid, 0.2 mL of 5% vanillin glacial acetic acid solution, and 1 mL of perchloric acid were added to 1 mL standard solutions, then placed in a 60 °C water bath for 15 min. After 10 min, 5 mL glacial acetic acid was added, then the absorbance value at 545 nm was measured and the standard curve was drawn. The absorbance value of the prepared isopropanol solution was measured by a similar method, and the total triterpenoid content was calculated according to the standard curve.

For determining flavonoid and polyphenol content, 1 g of plant dried powder was ground with 50 mL 50% ethanol, then transferred into centrifuge tubes and centrifuged at  $5000\times g$  for 20 min at 4 °C. Then, the crude extract of flavonoids and polyphenols was obtained through the rotation–evaporation method. The standard curve of total flavonoids was drawn with rutin as the standard, and the content of total flavonoids in the crude extract was determined by the classical  $\text{NaNO}_2$ – $\text{AlCl}_3$  spectrophotometry [46]. The standard curve of total polyphenols was drawn with gallic acid as the standard, and the content of total polyphenols in the crude extract was determined by classical  $\text{Na}_2\text{CO}_3$  Folin phenol spectrophotometry [47].

### 2.10. Statistical Analysis

All graphing and statistical analyses were performed using Origin Pro 2010 and all the heat maps were drawn with TBtools software. Data were statistically analyzed using the SPSS software version 19.0. Data in the text and tables are expressed as standard deviation means, and error bars in the figures indicate standard deviations. All statistical tests were subjected to ANOVA, the Wilcoxon signed rank test, and least-significant-difference using the  $p < 0.05$  significance level.

## 3. Results

### 3.1. Isolation of Endophytic Bacteria and Fungi from *S. sphenanthera*

A total of 127 bacterial and 119 fungal strains were isolated from the roots, stems, leaves, and fruits of *S. sphenanthera* (see Figure S1). Of these isolates, 27 bacterial and 26 fungal isolates belonging to diverse taxa were chosen for subsequent experiments (see Figures S2 and S3). These bacterial isolates represented four phyla, namely, Proteobacteria, Bacteroides, Actinobacteria, and Firmicutes. Fungal isolates represented three phyla, namely, Ascomycota, Basidiomycota, and Zygomycota. These bacterial and fungal strains identified from plant-associated organs are shown in Table 1.

**Table 1.** Representative endophytic bacterial and fungal strains isolated from *S. sphenanthera*.

| Bacteria       |                             |         | Fungi         |                              |         |
|----------------|-----------------------------|---------|---------------|------------------------------|---------|
| Phylum         | Genus                       | Numbers | Phylum        | Genus                        | Numbers |
| Firmicutes     | <i>Bacillus</i> sp.         | SLB12   | Ascomycota    | <i>Pestalotiopsis</i> sp.    | SRF21   |
| Firmicutes     | <i>Lysinibacillus</i> sp.   | SRB6    | Ascomycota    | <i>Trichoderma</i> sp.       | SSF13   |
| Firmicutes     | <i>Viridibacillus</i> sp.   | SFB11   | Ascomycota    | <i>Colletotrichum</i> sp.    | SSF14   |
| Firmicutes     | <i>Romboutsia</i> sp.       | SRB23   | Ascomycota    | <i>Fusarium</i> sp.          | SFF11   |
| Firmicutes     | <i>Straphylococcus</i> sp.  | SSB39   | Ascomycota    | <i>Lasiodiplodia</i> sp.     | SLF1    |
| Firmicutes     | <i>Enterococcus</i> sp.     | SLB1    | Ascomycota    | <i>Bipolaris</i> sp.         | SSF12   |
| Firmicutes     | <i>Brevibacillus</i> sp.    | SFB12   | Ascomycota    | <i>Penicillium</i> sp.       | SRF9    |
| Bacteroidetes  | <i>Flavobacterium</i> sp.   | SSB1    | Ascomycota    | <i>Diaporthe</i> sp.         | SLF18   |
| Bacteroidetes  | <i>Sphingobacterium</i> sp. | SRB12   | Ascomycota    | <i>Daldinia</i> sp.          | SLF4    |
| Bacteroidetes  | <i>Mucilaginibacter</i> sp. | SSB4    | Ascomycota    | <i>Neopestalotiopsis</i> sp. | SLF5    |
| Bacteroidetes  | <i>Wautersiella</i> sp.     | SSB19   | Ascomycota    | <i>Beltrania</i> sp.         | SLF21   |
| Bacteroidetes  | <i>Alloprevotella</i> sp.   | SLB9    | Ascomycota    | <i>Guignardia</i> sp.        | SLF6    |
| Actinobacteria | <i>Nocardioides</i> sp.     | SSB16   | Ascomycota    | <i>Phomopsis</i> sp.         | SFF9    |
| Actinobacteria | <i>Micrococcus</i> sp.      | SLB31   | Ascomycota    | <i>Botryosphaeria</i> sp.    | SRF16   |
| Actinobacteria | <i>Brevibacterium</i> sp.   | SLB15   | Ascomycota    | <i>Hypoxyylon</i> sp.        | SLF24   |
| Actinobacteria | <i>Kocuria</i> sp.          | SLB14   | Ascomycota    | <i>Eutypella</i> sp.         | SSF11   |
| Proteobacteria | <i>Pantoea</i> sp.          | SSB8    | Ascomycota    | <i>Hyphopichia</i> sp.       | SFF7    |
| Proteobacteria | <i>Burkholderia</i> sp.     | SRB18   | Basidiomycota | <i>Clitopilus</i> sp.        | SSF19   |
| Proteobacteria | <i>Serratia</i> sp.         | SFB13   | Basidiomycota | <i>Ceratobasidium</i> sp.    | SFF6    |
| Proteobacteria | <i>Xanthomonas</i> sp.      | SFB7    | Basidiomycota | <i>Phlebiopsis</i> sp.       | SSF18   |
| Proteobacteria | <i>Limnobacter</i> sp.      | SLB7    | Basidiomycota | <i>Emmia</i> sp.             | SFF12   |
| Proteobacteria | <i>Duganella</i> sp.        | SRB22   | Basidiomycota | <i>Irpex</i> sp.             | SRF17   |
| Proteobacteria | <i>Rhizobium</i> sp.        | SLB15   | Basidiomycota | <i>Phlebia</i> sp.           | SLF27   |
| Proteobacteria | <i>Agrobacterium</i> sp.    | SSB31   | Basidiomycota | <i>Perenniporia</i> sp.      | SLF26   |
| Proteobacteria | <i>Herbaspirillum</i> sp.   | SFB6    | Zygomycota    | <i>Umbelopsis</i> sp.        | SLF28   |
| Proteobacteria | <i>Stenotrophomonas</i> sp. | SSB25   | Zygomycota    | <i>Mucor</i> sp.             | SRF1    |
| Proteobacteria | <i>Enterobacter</i> sp.     | SLB11   |               |                              |         |

### 3.2. Isolation and Identification of Triterpenoids from *S. sphenanthera*

Four known schitriterpenoids (S1 and S2) and highly oxygenated schinortriterpenoids (S3 and S4), namely, iso-anwuweizic acid (S-1; C<sub>30</sub>H<sub>50</sub>O<sub>2</sub>), nigranoic acid (S2; C<sub>30</sub>H<sub>46</sub>O<sub>4</sub>), micrandilactone C (S3; C<sub>29</sub>H<sub>34</sub>O<sub>9</sub>), and lancifodilactone D (S4; C<sub>29</sub>H<sub>42</sub>O<sub>9</sub>), were obtained from the crude acetone extracts of dry plant organs from *S. sphenanthera* after successive separation and purification using various column chromatography methods (Figure 1). The structures of the known triterpenoids (S1–S4) were identified by comparing the NMR and MS data with those reported in the literature (Figures S12–S15) [48–51].

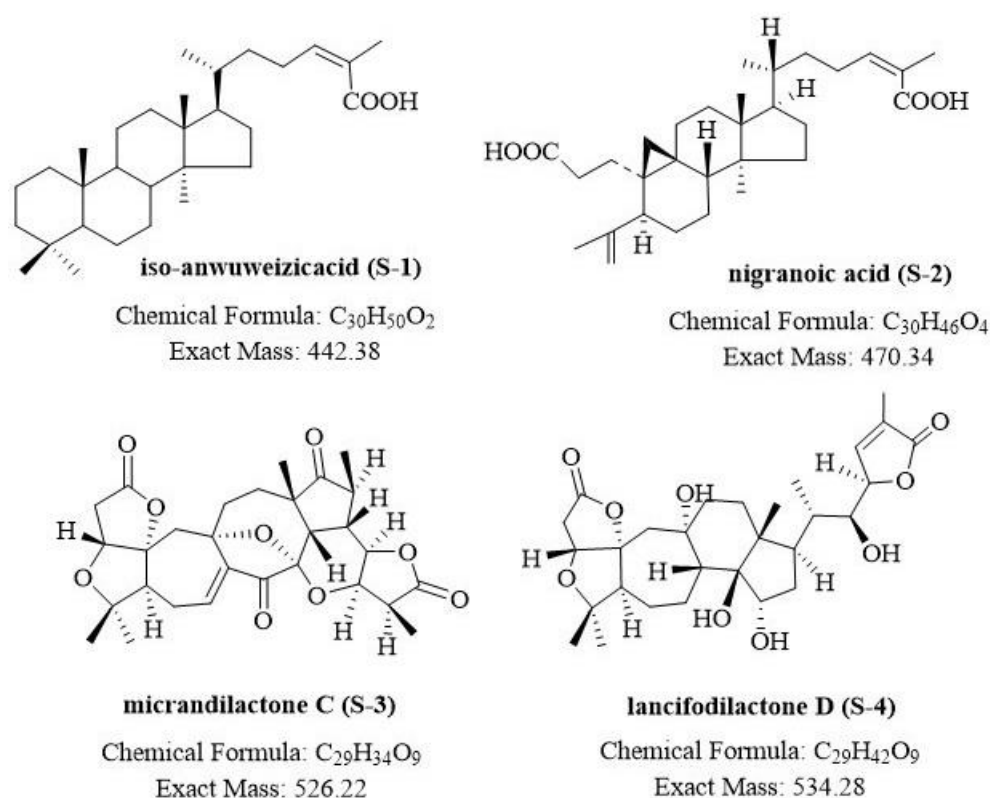


**Figure 1.** Structures of Schitriterpenoids and Schnortriterpenoids.

### 3.3. Effect of Triterpenoid Metabolites on the Growth of Endophytes

In order to evaluate the regulative effects of triterpenoid mixtures on the growth of endophytic strains, representative endophytic strains were cultured in a medium containing different initial concentrations of mixed triterpenoid metabolites and their growth was measured. Results indicated that the type of regulation, be it promotion or inhibition, mainly depended on the examined endophytic species and the involved concentrations of triterpenoid mixtures (Figure 2). All examined Actinobacteria isolates were grouped into TNB (bacteria growth-inhibited by triterpenoids), including *Kocuria* sp., *Micrococcus* sp. and *Nocardioides* sp. By contrast, four out of five Bacteroidetes isolates were grouped into TPB, which were *Flavobacterium* sp., *Sphingobacterium* sp., *Alloprevotella* sp., and *Mucilaginibacter* sp. However, for isolates belonging to Firmicutes, five out of eight Firmicutes isolates were grouped into TPB. For isolates belonging to Proteobacteria, only four out of eleven Proteobacteria isolates were grouped into TPB (Figures 2A and S4). Similarly, growth regulatory effects of triterpenoid mixtures were found in fungal strains (Figures 2B and S5). A relatively equal number of isolates belonging to Ascomycota and Basidiomycota were grouped into TPF (fungi growth-promoted by triterpenoids) and TNF (fungi growth-inhibited by triterpenoids). Eight of fifteen Ascomycota isolates were grouped into TPF, and three out of six Basidiomycota isolates were grouped into TPF.



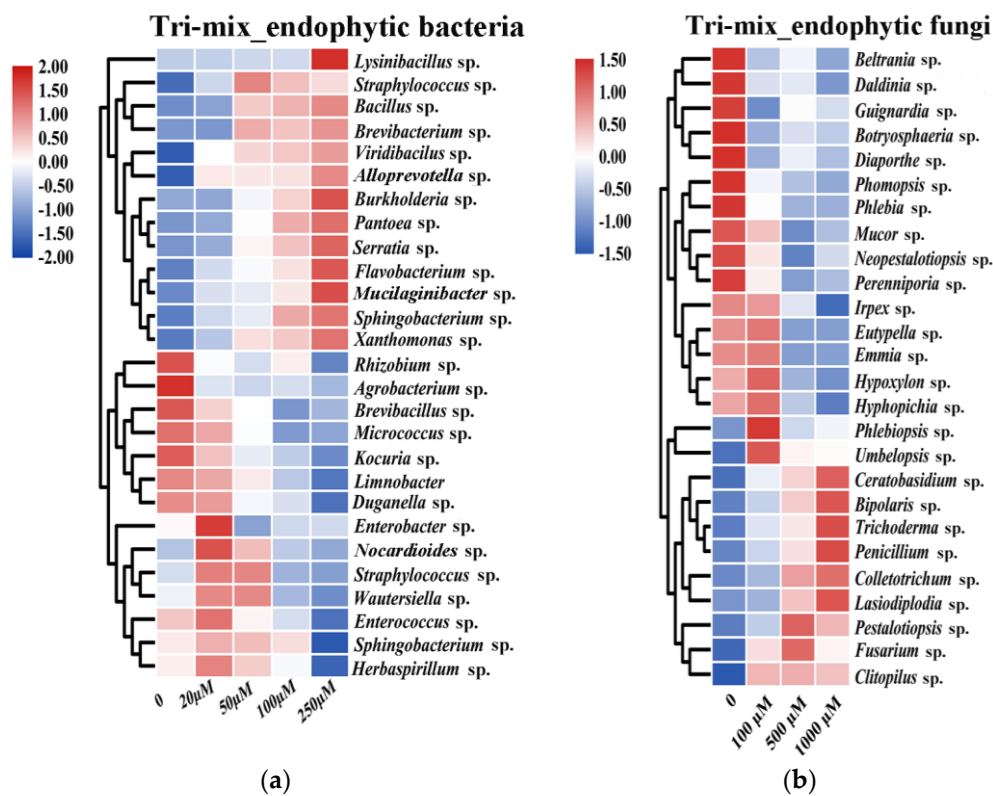


**Figure 2.** Effects of Triterpenoids on the growth of bacterial and fungal isolates. Heatmap showing log<sub>2</sub> fold change in (a) cell density (OD<sub>600</sub>) of bacterial strain and (b) weight (g) of fungal strain treated with mix (S1–4) by gradient concentration at 48 h (bacteria) and 12 days (fungi). Log<sub>2</sub> fold change is an estimate of the log<sub>2</sub> ratio of relative value to that initial value. A value of 1.0 indicates two-fold greater expression in heatmap cluster. Five biological replicates per treatment were used for analysis.

Two trends were observed in the growth-inhibited effect of triterpenoids on TNB strains, one of which was that the growth of TNB strains was progressively enhanced with the increase in mix concentration, such as in *Straphylococcus* sp., *Bacillus* sp. and *Brevibacterium* sp. The other was slightly promoted by low concentrations of the mix (20 and 50 μM) and significantly inhibited by medium to high concentrations of the mix (100 and 250 μM), such as in *Enterobacter* sp., *Nocardioides* sp. and *Straphylococcus* sp. (Figures 2A and S4). By contrast, the growth-inhibited effect of triterpenoids on TNF strains gradually increased with the increase in mix concentration, such as in *Trichoderma* sp., *Penicillium* sp., and *Colletotrichum* sp. (Figures 2B and S5). Overall, triterpenoids showed selective growth regulation to endophytic bacteria and fungi.

### 3.4. Functional Screening of Endophytes

The representative endophytic strains of diverse taxa were screened with plant growth promotion traits (PGPT). Among bacterial genera, Indole acetic acid (IAA) production tended to be stronger in the bacterial isolates of genera *Sphingobacterium* sp. (66.3 mg/L) and *Kocuria* sp. (66.3 mg/L) than in other isolates. Contrarily, isolates of *Straphylococcus* sp. and *Enterococcus* sp. did not produce IAA. All tested isolates exhibited antioxidative activity, and the isolate with the highest DPPH radical scavenging capacity was the genus of *Enterococcus* sp. (89.7%). Production of P-solubilization was particularly high in genera *Serratia* sp. (137.8 mg/L) and *Lysinibacillus* sp. (129.7 mg/L). *Enterobacter* sp. and *Bacillus* sp. were also strong producers of siderophores, whereas most other tested isolates produced only trace amounts of or no siderophores (see Table S1). For fungi, the overall share of IAA-producing fungi in our study was also much lower compared to that of bacteria. Isolates of *Lasiodiplodia* sp. (19.1 mg/L) displayed the highest IAA production. We also found that *Penicillium* sp. (175.6 mg/L) and *Perenniporia* sp. (175.6 mg/L) were the most

prominent P-solubilizing producers, followed by *Phlebiopsis* sp. (159.4 mg/L) and *Irpex* sp. (157.6 mg/L). Fungal isolates exhibited high antioxidative activity, with 7 of 26 tested fungal isolates at the level of  $\geq 90\%$ . *Penicillium* sp. (53.5 mg/L) and *Pestalotiopsis* sp. (51.0 mg/L) were the strongest producers of siderophores (see Table S2).

Combining PGPT with the growth-regulating effect of triterpenoids on these endophytes indicated that the PGPT ability of TPB and TPF was significantly higher than that of TNB and TNF. Functional overlaps were common in these microbes, with most TPB and TPF strains possessing one, two, or three PGPT abilities (Figure 3A,B).

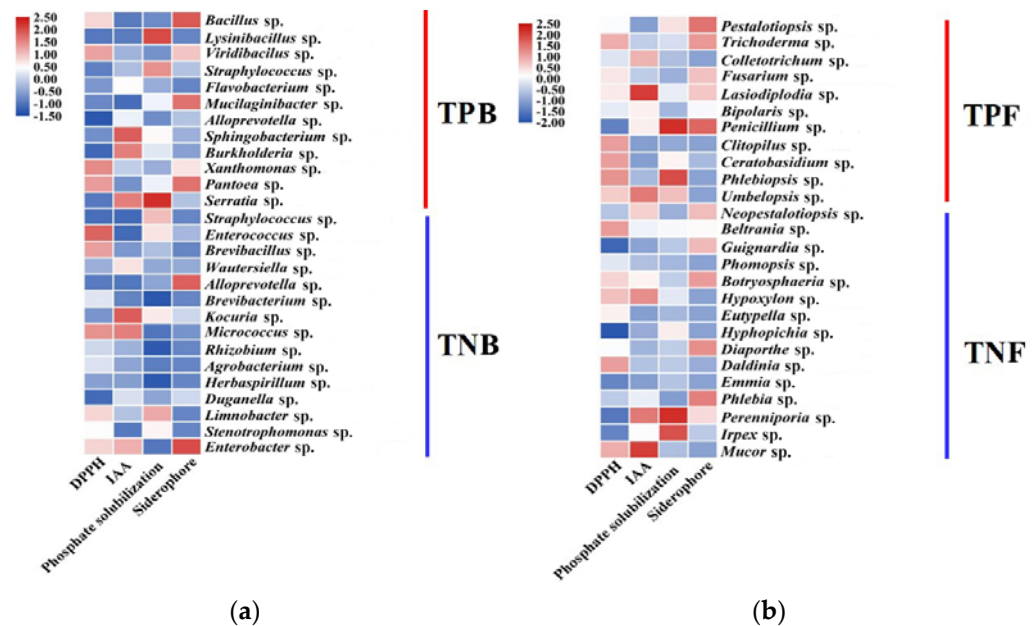


**Figure 3.** Plant growth promotion traits (PGPT) and triterpenoid synthesis capacity of representative bacterial and fungal isolates. (a) Heatmap of PGPT of 27 endophytic bacterial isolates. (b) Heatmap of PGPT of 26 endophytic fungal isolates. Three biological replicates per treatment were used for analysis.

### 3.5. Plate Interaction Showed TPB and TPF Are More Important in the Interaction Network

To understand whether and how these TPB and TPF strains might modulate microbial communities in Schisandraceae plants, we also tested 1951 binary interactions in vitro with diverse taxa of 27 bacterial and 26 fungal isolates from our culture collection. The growth of most bacteria was promoted by the bacteria belonging to the isolates of *Bacillus* sp., *Burkholderia* sp., *Sphingobacterium* sp., *Mucilagibacter* sp., and *Flavobacterium* sp. On the contrary, the growth of most bacteria was inhibited by bacteria belonging to the isolates of *Rhizobium* sp., *Agrobacterium* sp., *Herbaspirillum* sp., *Micrococcus* sp., *Enterobacter* sp., *Limnobacter* sp., and *Duganella* sp. (Figures 4A and S8). Several fungi, such as *Neopestalotiopsis* sp., *Umbelopsis* sp., *Fusarium* sp., and *Phlebia* sp., promoted most of the other fungi, yet fungi belonging to *Trichoderma* sp., *Ceratobasidium* sp., *Lasioidiplodia* sp., and *Clitopilus* sp. inhibited most other fungi (Figures 4B and S9). However, inhibited effects existed between most bacteria and fungi, including several bacterial strains belonging to the *Bacillus* sp., *Viridibacillus* sp., *Pantoea* sp., and *Duganella* sp., which exhibited high inhibitory effects on other fungal isolates (Figures 4C and S10). Above all, the binary interaction phenotypes determined in the microbial interaction screen revealed that most mutual inhibition occurs between bacteria and fungi, and cooperation in the bacterial and fungal communities occurs more than competition.

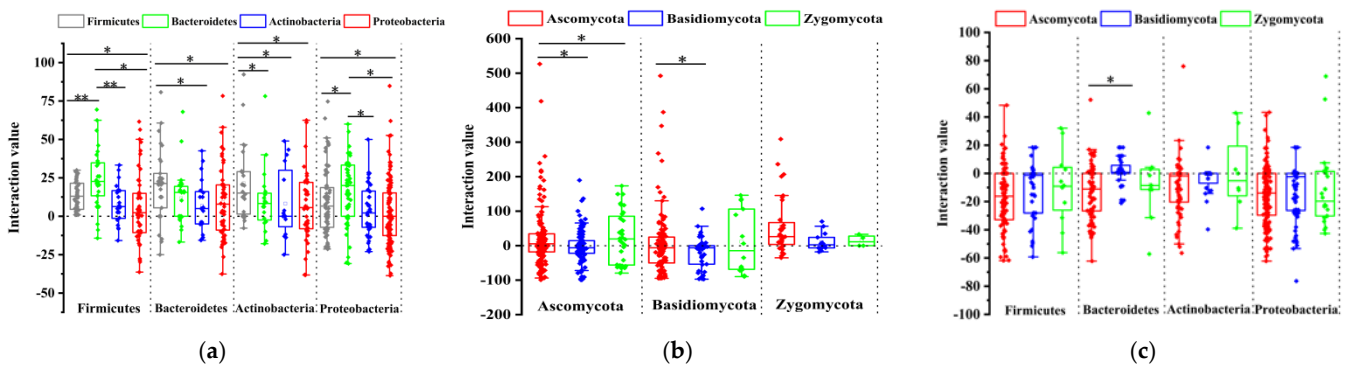


**Figure 4.** Interactions of representative bacterial and fungal isolates. (a) Box-plot analysis of endophytic bacterial interactions at the taxonomic level of the phylum. (b) Box-plot analysis of endophytic fungal interactions at the taxonomic level of the phylum. (c) Box-plot analysis of the interaction between endophytic bacteria and fungi at the taxonomic level of the phylum. Asterisks indicate significant differences between the group: \*\*  $p < 0.01$ , \*  $p < 0.05$ , nonparametric test, Wilcoxon signed rank test. Three biological replicates per treatment were used for analysis. Error bars represent the SEM.

Combining the interaction strength with the growth-regulating effect of triterpenoids on these endophytes indicated that TPB strains were more promoted by the bacterial community than TNB strains (Figure 5A). However, no significant differences were observed between TPF and TNF strains (Figure 5B). TPF strains *Trichoderma* sp., *Lasiodiplodia* sp., *Clitopilus* sp., and *Ceratobasidium* sp. significantly inhibited the growth of other endophytic fungi (Figure S9). Similar to bacterial results, less inhibition from the bacterial community was observed in TPF strains compared with TNF strains (Figure 5C). These results indicated that triterpenoids could promote the endophytic strains that show more dominance in community interactions.

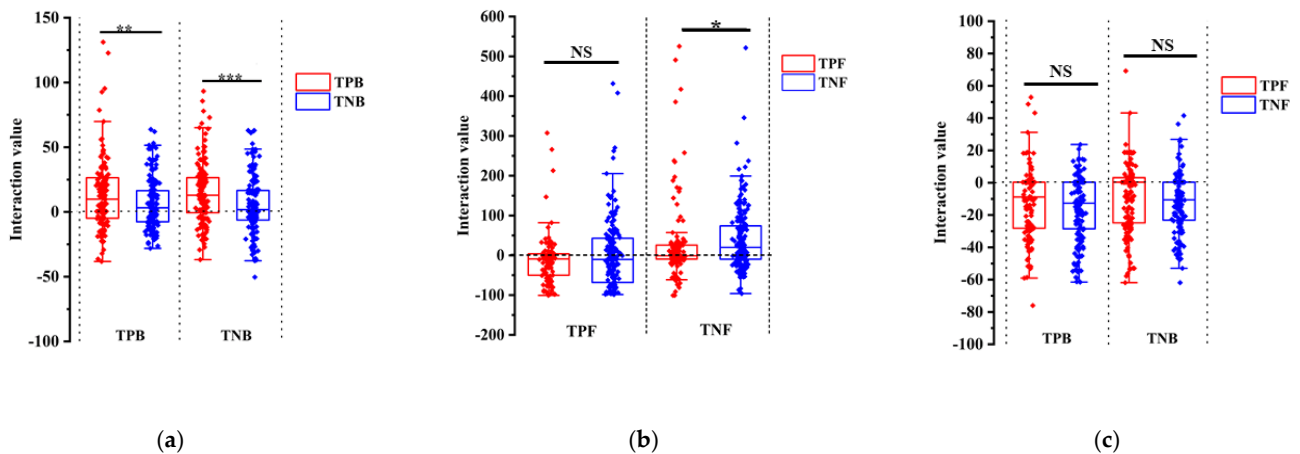


**Figure 5.** Correlation analysis between growth regulation effect of triterpenoids and the interaction. (a) Correlation analysis between growth regulation effect of triterpenoids on endophytic bacteria and the interaction of endophytic bacteria. (b) Correlation analysis between growth regulation effect of triterpenoids on endophytic fungi and the interaction of endophytic fungi. (c) Correlation analysis between growth regulation effect of triterpenoids on endophytes and the interaction between endophytes. Asterisks indicate significant differences between the group: \*\*\*  $p < 0.001$ , \*\*  $p < 0.01$ , \*  $p < 0.05$ , nonparametric test, Wilcoxon signed rank test. Three biological replicates per treatment were used for analysis. Error bars represent the SEM.

### 3.6. Evaluation of SynComs

To further investigate the performance of the microbial consortium promoted by triterpenoids, pot experiments were carried out in the growth chambers. By using microbes that were diverse taxa of 27 bacterial and 26 fungal isolates from our culture collection, we constructed six SynComs (synthetic microbial communities) consisting of 27 bacteria (AB), 26 fungi (AF), 27 bacteria and 26 fungi (ABF), 14 growth-inhibited bacteria and

15 growth-inhibited fungi by triterpenoid (TNB&TNF), 13 growth-promoted bacteria and 11 growth-promoted fungi by triterpenoid (TPB&TPF), or control check (CK). In this test, SEM results showed that a large number of endophytic bacteria and endophytic fungi were observed in the roots of TPB&TPF plants compared with CK plants (Figure 6), which proved that the co-culture system was effective for subsequent study. We then explored whether the SynComs could influence plant growth and metabolic accumulation.

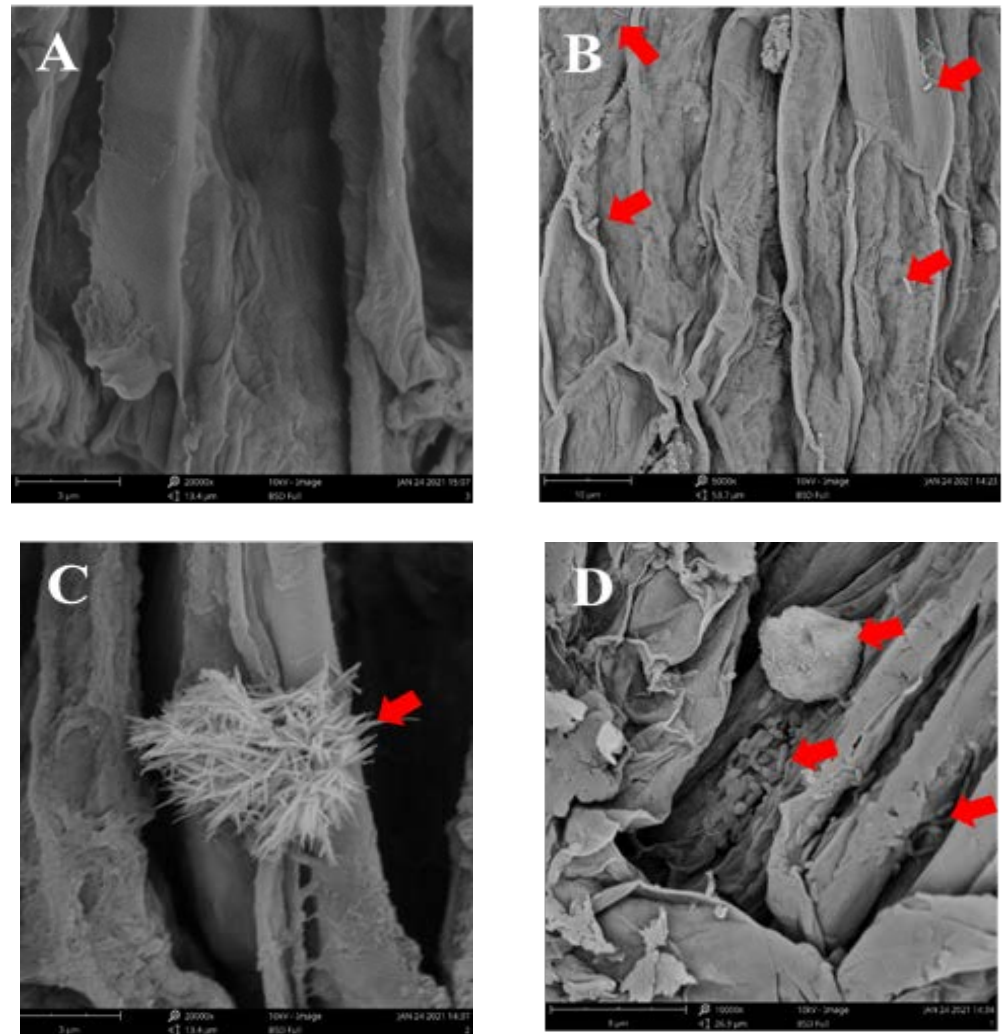
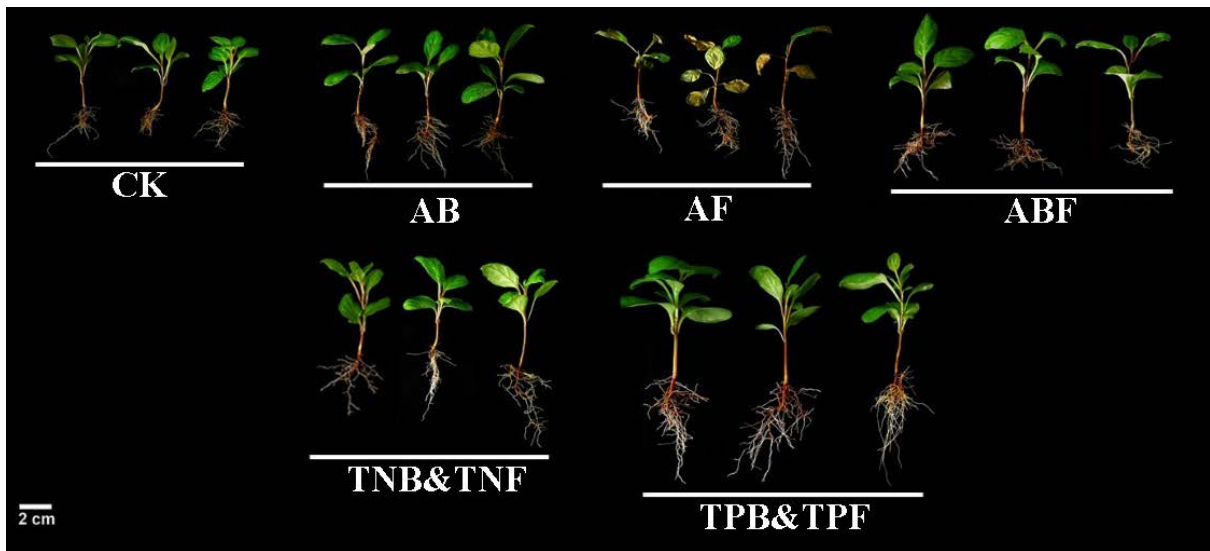


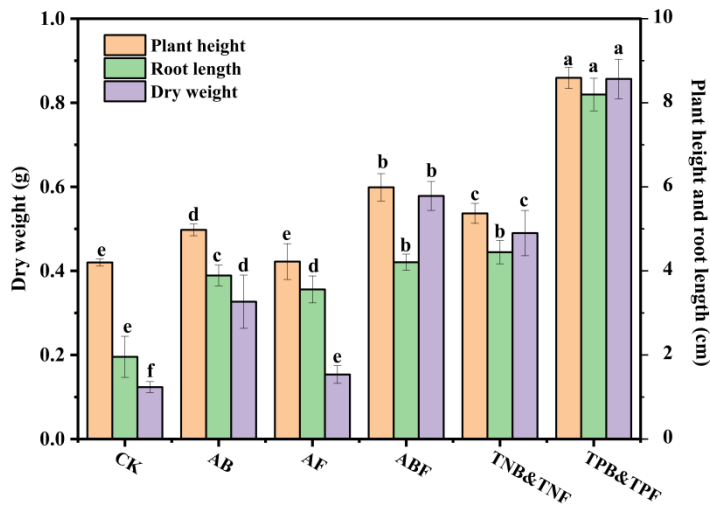
**Figure 6.** Colonization of *S. sphenanthera* roots by bacteria and fungi in different treatment groups. (A) Roots of *S. sphenanthera* in control group, in which no microbes were found. (B) Roots of *S. sphenanthera* in AB, in which red arrow represents colonized bacteria. (C) Roots of *S. sphenanthera* in AF, in which red arrow represents colonized fungi. (D) Roots of *S. sphenanthera* in ABF group, in which red arrow represents coexistence of colonized bacteria and fungi.

Plants inoculated with AB, AF, and ABF significantly promoted *S. sphenanthera* growth, as indicated by a 98.96%, 82.02%, and 115.00% increase in root length, and a 18.45%, 4.49%, and 42.55% increase in plant height, respectively, in comparison with the control plants (Figure 7B). In addition, in comparison with groups AB and AF, the ABF group had significant effects on the growth of *S. sphenanthera*, indicating that endophytic bacteria and fungi had synergistic effects in promoting the growth of *S. sphenanthera*. Moreover, the group of TPB&TPF further promoted the growth of plants, as indicated by a 203.98% and 61.98% root length and plant height increase, respectively, in comparison with the ABF group, whereas the group of TNB&TNF showed insignificant improvement in the growth of plants, as indicated by a 5.73% increase and a 10.3% reduction in root length

and plant height, respectively, in comparison with the ABF group (Figure 7B). Further experimentation with SynComs TPB&TPF and TNB&TNF suggested that the microbes promoted by triterpenoids could promote plant growth by increasing root length and plant height. In addition, plants inoculated with AF had a wilt pathogen in the leaves (Figure 7A), as indicated by a 42.18% decrease in the chlorophyll content of the leaves (Figure 8A), indicating that the existence of endophytic bacteria is helpful in reducing the toxic effect of endophytic fungi on plants.



(a)



(b)

**Figure 7.** Pot experiment of SynCom in germ-free *S. sphenanthera* plants. (a) Growth status of *S. sphenanthera* in different treatment groups. (b) Effects of different SynComs on root length, stem length, and dry weight of *S. sphenanthera*. Different lowercase letters (a–f) indicate significant differences between different treatments, one-way ANOVA, Duncan’s test. Error bars represent the SEM.

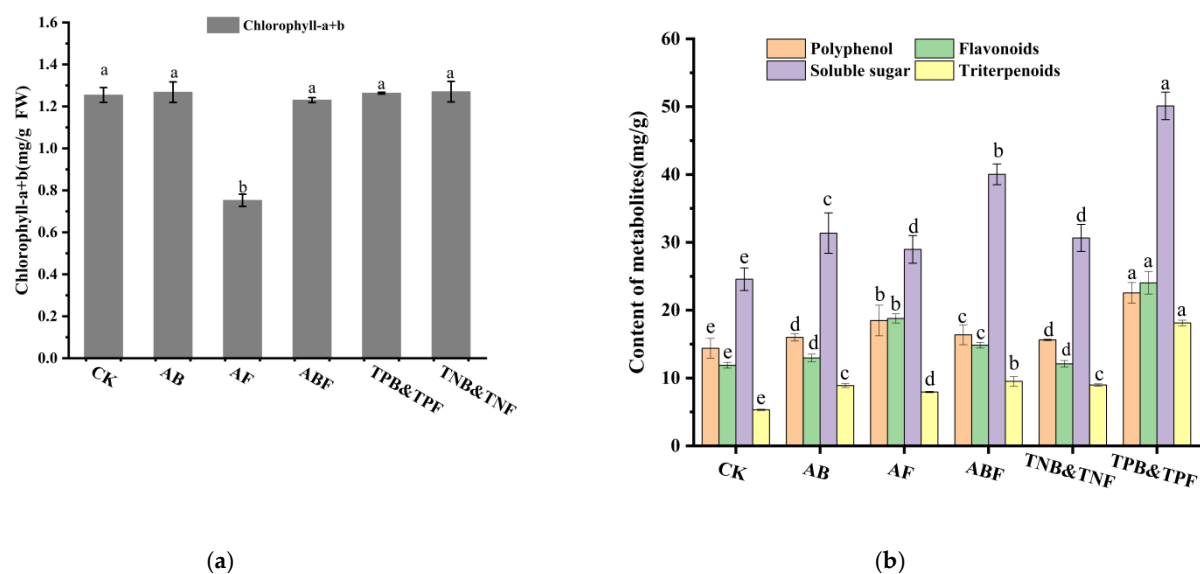


**Figure 8.** Effects of different SynComs on the contents of metabolites in *S. sphenanthera*. (a) Effects of different SynComs on contents of total sugar, flavonoids, polyphenols, and total terpenoid in *S. sphenanthera*. (b) Effects of different SynComs on the chlorophyll content of *S. sphenanthera*. Different lowercase letters (a–e) indicate significant differences between different treatments, one-way ANOVA, Duncan’s test. Error bars represent the SEM.

Polyphenols, flavonoids, total sugars, and total triterpenoids are the main metabolites in *S. sphenanthera*. Here, the content of metabolites was determined to evaluate the effects of six SynComs on the metabolic accumulation of *S. sphenanthera*. The polyphenol content increased by 11.12%, 28.37%, 13.76%, 8.56%, and 56.66%; the flavonoid content increased by 9.16%, 58.13%, 25.00%, 8.60%, and 102.21%; the total sugar content increased by 27.66%, 17.87%, 62.91%, 24.75%, and 103.96%; the total triterpenoid content increased by 66.97%, 49.13%, 78.78%, 68.51%, and 240.54% for SynCom AB, AF, ABF, TNB&TNF, and TPB&TPF-treated hosts, respectively (Figure 8B). Results show that all five SynComs could promote metabolite accumulation in the host plants, among which SynCom TPB&TPF accumulated significantly more metabolites of *S. sphenanthera* than the four other SynComs.

#### 4. Discussion

Secondary metabolites are a promising target for rationally manipulating the plant microbiome because these molecules frequently exhibit the function of regulating microbes [12]. Specifically selected microbial groups often have special physiological functions for plants. Microbial groups that are specifically regulated by these compounds play an important role in the growth, nutrient absorption, and defense of the host plant [8–11]. Recent reports have demonstrated that plant secondary metabolites can affect and regulate rhizosphere microbial composition through rhizosphere secretion, including triterpenoids, glucosinolates, flavonoids, phytoalexin, benzoxazines, and coumarins. The mutualistic relationship between plant and endophyte is due to the adaptation and utilization of host secondary metabolites by the endophyte. Thus, we speculated that secondary metabolites were important factors for the enrichment of the microbial community.

Since *S. sphenanthera* is an important medicinal plant that can produce diverse schitriterpenoids [26,27], we tested the hypotheses that triterpenoid-rich medicinal plant *S. sphenanthera* could recruit beneficial endophytic bacteria and fungi through triterpenoids. In our research for the triterpenoid-mediated effects on endophytic microbiome assembly, in vitro traits of the culturable endophytes in *S. sphenanthera* using different concentrations of triterpenoids confirmed these triterpenoids had selective activity on endophytes. First, at the phylum level, the in vitro growth of most Firmicutes, Bacteroides, and some Proteobacteria, Ascomycota, and Basidiomycota was generally promoted by triterpenoids, whereas the growth of most Actinobacteria, and some Proteobacteria, Ascomycota, and Basidiomycota

was generally inhibited by triterpenoids. This finding demonstrated that triterpenoids play an important regulatory role in endophytic communities of *S. sphenanthera*. Moreover, the endophytic fungus *Penicillium* sp., which was significantly promoted by triterpenoids, was able to convert and modify host triterpenoids in our previous findings [28]. Previous studies showed that endophytic fungi from *Armoracia rusticana* could decompose glucosinolates by utilizing them as a carbon source [52]. Another study on *Cephalotaxus harringtonia* also showed that endophytic fungus *Paraconiothyrium variabile* could transform the host metabolites of glycosylated flavonoids, and the deglycosylated flavonoids displayed beneficial effects on the hyphal growth of germinated spores [53]. This suggested that the endophytes show adaptation to the host plant's secondary metabolites and are controlled by plant metabolites. Therefore, we speculated that the regulatory relationship of triterpenoids to endophytes is due to the utilization and metabolism of triterpenoids by endophytes.

Our results based on the analysis of the interaction between endophytic bacteria and fungi in vitro showed that more mutual promotion existed within the group of bacteria and within the group of fungi, and more mutual inhibition existed between the two groups. These results suggest that the whole endophytic microbial community maintained a relatively balanced state. Similarly, a previous study on the root microbiome of *Arabidopsis thaliana* suggested that filamentous fungi are harmful to the health and survival of plants without bacterial competitors [41]. Bacteria of many genera had significant antagonism to endophytic fungi; species such as *Bacillus* sp., *Viridibacillus* sp., *Pantoea* sp., *Duganella* sp., and *Sphingobacterium* sp. display the strongest antagonistic ability against fungal species. Consistently, these genera could protect plants from pathogens [54–57]. These results provide a reasonable framework to explain why these strains are widely used in plant biological control in agricultural environments. Some species of *Pantoea* sp. have long been recognized as phytopathogens that can cause diseases of crops and forest trees, whereas some endophytic *Pantoea* sp. show antagonistic abilities against some plant pathogens [58]. This suggests that strains belonging to the same genus may play different roles in various host plants and environments. In total, the balance of endophytic microbial groups in *S. sphenanthera* is not determined by the interaction of a single class, but by the interaction of multi-kingdom microbial consortia, which is conducive to the healthy growth of plants.

Great attention is paid to the endophytes, as they contribute to plant fitness and productivity by providing a plethora of functional capacities, and there is increasing interest in using synthetic communities of microbial strains to promote plant growth fitness and metabolites. Previous studies on soybean plants suggested that constructed synthetic microbial communities based on functional screening were capable of enhancing nutrient acquisition and crop yield through the activities of beneficial root-associated microbes [14]. Currently, these are few guiding principles for constructing SynComs. These include methods to construct synthetic communities according to plant-growth-promotion traits [14], the functional features of individual strains [39], and OTU screening based on high-throughput sequencing [22]. The relationship between secondary metabolites and the microbiome can provide a new tool for the rational manipulation of the plant microbiome [11]. In our study, we considered the effects of triterpenoids on strains and the balance between bacteria and fungi for the construction of SynComs. We grew *S. sphenanthera* plants in soils preinoculated with the six SynComs described in the results to test for their ability to affect plant growth and health. Our results suggest that the inoculation of plants with bacterial communities significantly reverses fungi's harm for the plant to promote plant growth, health, and metabolic accumulation. Microbial consortia composed of TPB and TPF could significantly promote plant growth, root development, and metabolic accumulation, suggesting that they also synergistically promote the growth of host plants. Among TPB and TPF isolates, some species of *Lysinibacillus* sp., *Brevibacterium* sp., *Colletotrichum* sp., and *Clitopilus* sp. were confirmed to be members of plant-growth-promoting strains [2,58–60]. *Ceratobasidium* sp. was capable of facilitating metabolic accumulation in host plants, such as the medicinal plant *Anoectochilus roxburghii* [61]. Some endophytic *Bacillus* sp., *Xanthomonas* sp., *Pantoea* sp., *Trichoderma* sp., and *Fusarium* sp. were

treated as an effective bio-control agent against phytopathogenic fungi [20,54–56,62–68]. As a consortium, the microbes promoted by triterpenoids are beneficial to the plant, as they can unite the inter-kingdom and the outer-kingdom microbial consortia, and also promote plant growth. These findings together show that *S. sphenanthera* rich in triterpenoids could recruit specific members of their microbes to aid in their growth, health, and metabolic accumulation. Our results suggest that it is a feasible method for plant growth and metabolism accumulation to construct synthetic communities of bacteria and fungi based on basis of triterpenoid selection.

## 5. Conclusions

We isolated endophytic bacteria and fungi from the plant organs of *S. sphenanthera*, which were assayed by the purified triterpenoids and filtered to construct SynComs on the basis of triterpenoid screening. Our work suggests that triterpenoids, other than their wide biological activity, may play a role in the assembly and stabilization of the plant's endophytic microbiome. Moreover, the SynComs of endophytes based on the screening of triterpenoids could significantly promote the growth and metabolic accumulation of plants. Our findings demonstrate that triterpenoids play an important regulatory role in endophytic communities of *S. sphenanthera*. Furthermore, these findings provide insights into how plant secondary metabolites affect their endophytic microbial community and how the endophytic bacteria and fungi coexist in plants, providing new approaches to construct SynCom in *S. sphenanthera* which may open new avenues towards the breeding of high-yielding and high metabolite-accumulating medicinal plants by exploiting their interaction with beneficial endophytes.

**Supplementary Materials:** The following are available online at <https://www.mdpi.com/article/10.3390/jof7100788/s1>, Figure S1: Morphological pictures of roots, stems, leaves, and fruits of *S. sphenanthera*, Figure S2: Morphological pictures of some representative endophytic bacteria and fungi from *S. sphenanthera*, Figure S3: Phylogenetic relationships of representative endophytic bacteria and fungi from *S. sphenanthera*. Figure S4: Growth curve of endophytic bacteria under different mix concentrations. Error bars represent the SEM. Figure S5: Effects of different concentrations of mix on the growth of endophytic fungi. Different lowercase letters (a, b, c, and d) indicate significant differences between different treatments, one-way ANOVA, Duncan test. Error bars represent the SEM. Figure S6: Diagram of plate interaction of endophytic bacteria and fungi. Figure S7: Plate interaction between representative endophytes. Figure S8: Cluster analysis heat map of interactions at the taxonomic level of the bacterial genus. Figure S9: Cluster analysis heat map of interactions at the taxonomic level of the fungal genus. Figure S10: Cluster analysis heat map of interactions at the taxonomic level between the bacterial and fungal genus. Figure S11: Co-culture system of synthetic communities and *S. sphenanthera*. Table S1: Isolation culture media of endophytic bacteria and fungi. Table S2: Plant growth promoting ability of representative endophytic bacteria. Table S3: Plant growth promoting ability of 26 representative endophytic fungi. Table S4: manufacturers of chemicals and solvents. Table S5: list of abbreviations.

**Author Contributions:** C.Y., J.D., and D.Q. conceived and designed the experiments. Y.W., B.Y., and Y.P. conducted the lab experiments and wrote the paper. J.X., W.L., and Y.L. edited the paper. All authors have read and agreed to the published version of the manuscript.

**Funding:** This research was funded by the National Natural Science Foundation of China [grant numbers 31270091, 20762015] and the Natural Science Foundation of Chongqing [grant numbers cstc20 18jcyjA0864].

**Institutional Review Board Statement:** Not applicable.

**Informed Consent Statement:** Not applicable.

**Data Availability Statement:** Genome accession numbers for the bacterial and fungal strains sequenced in this study were deposited in GenBank under accession numbers MZ707882-MZ707908 and MZ710145-MZ710170.



**Acknowledgments:** This work was financially supported by the National Natural Science Foundation of China [grant numbers 31270091, 20762015], the Natural Science Foundation of Chongqing [grant numbers cstc2018jcyjA0864].

**Conflicts of Interest:** The authors declare no conflict of interest.

## References

- Dini-Andreote, F. Endophytes: The second layer of plant defense. *Trends Plant Sci.* **2020**, *25*, 4. [[CrossRef](#)] [[PubMed](#)]
- Hiruma, K.; Gerlach, N.; Sacristan, S.; Nakano, R.T.; Hacquard, S.; Kracher, B.; Neumann, U.; Ramírez, D.; Bucher, M.; O’Connell, R.J.; et al. Root Endophyte Colletotrichum tofielliae Confers Plant Fitness Benefits that Are Phosphate Status Dependent. *Cell* **2016**, *165*, 464–474. [[CrossRef](#)] [[PubMed](#)]
- Matsumoto, H.; Fan, X.; Wang, Y.; Kusstatscher, P.; Duan, J.; Wu, S.; Chen, S.; Qiao, K.; Wang, Y.; Ma, B.; et al. Bacterial seed endophyte shapes disease resistance in rice. *Nat. Plants* **2021**, *7*, 60–72. [[CrossRef](#)] [[PubMed](#)]
- Paul, K.; Saha, C.; Nag, M.; Mandal, D.; Naiya, H.; Sen, D.; Mitra, S.; Kumar, M.; Bose, D.; Mukherjee, G.; et al. A Tripartite Interaction among the Basidiomycete *Rhodotorula mucilaginosa*, N<sub>2</sub>-Fixing Endobacteria, and Rice Improves Plant Nitrogen Nutrition. *Plant Cell* **2019**, *32*, 486–507. [[CrossRef](#)]
- Zheng, Y.; Gong, X. Niche differentiation rather than biogeography shapes the diversity and composition of microbiome of *Cycas panzhihuaensis*. *Microbiome* **2019**, *7*, 1–19. [[CrossRef](#)]
- Lopez, B.R.; Tinoco-Ojanguren, C.; Bacilio, M.; Mendoza, A.; Bashan, Y. Endophytic bacteria of the rock-dwelling cactus *Mammillaria fraileana* affect plant growth and mobilization of elements from rocks. *Environ. Exp. Bot.* **2012**, *81*, 26–36. [[CrossRef](#)]
- Jacoby, R.P.; Koprivova, A.; Kopriva, S. Pinpointing secondary metabolites that shape the composition and function of the plant microbiome. *J. Exp. Bot.* **2020**, *72*, 57–69. [[CrossRef](#)] [[PubMed](#)]
- Huang, A.C.; Jiang, T.; Liu, Y.-X.; Bai, Y.-C.; Reed, J.; Qu, B.; Goossens, A.; Nützmann, H.-W.; Bai, Y.; Osbourn, A. A specialized metabolic network selectively modulates Arabidopsis root microbiota. *Science* **2019**, *364*, eaau6389. [[CrossRef](#)]
- Stringlis, I.A.; Yu, K.; Feussner, K.; de Jonge, R.; Van Bentum, S.; Van Verk, M.C.; Berendsen, R.L.; Bakker, P.A.H.M.; Feussner, I.; Pieterse, C.M.J. MYB72-dependent coumarin exudation shapes root microbiome assembly to promote plant health. *Proc. Natl. Acad. Sci. USA* **2018**, *115*, E5213–E5222. [[CrossRef](#)]
- Koprivova, A.; Schuck, S.; Jacoby, R.P.; Klinkhammer, I.; Welter, B.; Leson, L.; Martyn, A.; Nauen, J.; Grabenhorst, N.; Mandelkow, J.F.; et al. Root-specific camalexin biosynthesis controls the plant growth-promoting effects of multiple bacterial strains. *Proc. Natl. Acad. Sci. USA* **2019**, *116*, 15735–15744. [[CrossRef](#)] [[PubMed](#)]
- Kudjordjie, E.N.; Sapkota, R.; Steffensen, S.K.; Fomsgaard, I.S.; Nicolaisen, M. Maize synthesized benzoxazinoids affect the host associated microbiome. *Microbiome* **2019**, *7*, 1–17. [[CrossRef](#)]
- Jacoby, R.P.; Chen, L.; Schwier, M.; Koprivova, A.; Kopriva, S. Recent advances in the role of plant metabolites in shaping the root microbiome. *F1000Research* **2020**, *9*, 151. [[CrossRef](#)]
- Zhalnina, K.; Louie, K.B.; Hao, Z.; Mansoori, N.; da Rocha, U.N.; Shi, S.; Cho, H.; Karaoz, U.; Loqué, D.; Bowen, B.P.; et al. Dynamic root exudate chemistry and microbial substrate preferences drive patterns in rhizosphere microbial community assembly. *Nat. Microbiol.* **2018**, *3*, 470–480. [[CrossRef](#)]
- Wang, C.; Li, Y.; Li, M.; Zhang, K.; Ma, W.; Zheng, L.; Xu, H.; Cui, B.; Liu, R.; Yang, Y.; et al. Functional assembly of root-associated microbial consortia improves nutrient efficiency and yield in soybean. *J. Integr. Plant Biol.* **2021**, *63*, 1021–1035. [[CrossRef](#)]
- Zarraonaindia, I.; Owens, S.; Weisenhorn, P.; West, K.; Hampton-Marcell, J.; Lax, S.; Bokulich, N.A.; Mills, D.A.; Martin, G.; Taghavi, S.; et al. The Soil Microbiome Influences Grapevine-Associated Microbiota. *mBio* **2015**, *6*, e02527-14. [[CrossRef](#)]
- Coleman-Derr, D.; Desgarennes, D.; García, C.F.; Gross, S.; Clingenpeel, S.; Woyke, T.; North, G.; Visel, A.; Partida-Martinez, L.P.; Tringe, S.G. Plant compartment and biogeography affect microbiome composition in cultivated and native *Agave* species. *New Phytol.* **2015**, *209*, 798–811. [[CrossRef](#)] [[PubMed](#)]
- De Souza, R.S.C.; Okura, V.K.; Armanhi, J.; Jorrín, B.; Lozano, N.; Da Silva, M.J.; Gonzalez-Guerrero, M.; De Araújo, L.M.; Verza, N.C.; Bagheri, H.C.; et al. Unlocking the bacterial and fungal communities assemblages of sugarcane microbiome. *Sci. Rep.* **2016**, *6*, 28774. [[CrossRef](#)] [[PubMed](#)]
- Hamonts, K.; Trivedi, P.; Garg, A.; Janitz, C.; Grinyer, J.; Holford, P.; Botha, F.C.; Anderson, I.C.; Singh, B.K. Field study reveals core plant microbiota and relative importance of their drivers. *Environ. Microbiol.* **2017**, *20*, 124–140. [[CrossRef](#)] [[PubMed](#)]
- Singh, B.K.; Millard, P.; Whiteley, A.; Murrell, J. Unravelling rhizosphere–microbial interactions: Opportunities and limitations. *Trends Microbiol.* **2004**, *12*, 386–393. [[CrossRef](#)]
- Berendsen, R.L.; Vismans, G.; Yu, K.; Song, Y.; de Jonge, R.; Burgman, W.P.; Burmølle, M.; Herschend, J.; Bakker, P.A.H.M.; Pieterse, C.M.J. Disease-induced assemblage of a plant-beneficial bacterial consortium. *ISME J.* **2018**, *12*, 1496–1507. [[CrossRef](#)] [[PubMed](#)]
- Hu, J.; Wei, Z.; Friman, V.-P.; Gu, S.-H.; Wang, X.-F.; Eisenhauer, N.; Yang, T.-J.; Ma, J.; Shen, Q.-R.; Xu, Y.-C.; et al. Probiotic Diversity Enhances Rhizosphere Microbiome Function and Plant Disease Suppression. *mBio* **2016**, *7*, e01790-16. [[CrossRef](#)] [[PubMed](#)]
- Zhuang, L.; Li, Y.; Wang, Z.; Yu, Y.; Zhang, N.; Yang, C.; Zeng, Q.; Wang, Q. Synthetic community with six *Pseudomonas* strains screened from garlic rhizosphere microbiome promotes plant growth. *Microb. Biotechnol.* **2020**, *14*, 488–502. [[CrossRef](#)] [[PubMed](#)]

23. Huang, W.; Long, C.; Lam, E. Roles of Plant-Associated Microbiota in Traditional Herbal Medicine. *Trends Plant. Sci.* **2018**, *23*, 559–562. [[CrossRef](#)]
24. Liu, Y.-X.; Qin, Y.; Bai, Y. Reductionist synthetic community approaches in root microbiome research. *Curr. Opin. Microbiol.* **2019**, *49*, 97–102. [[CrossRef](#)] [[PubMed](#)]
25. Liu, Y.; Zhu, A.; Tan, H.; Cao, L.; Zhang, R. Engineering banana endosphere microbiome to improve Fusarium wilt resistance in banana. *Microbiome* **2019**, *7*, 1–15. [[CrossRef](#)] [[PubMed](#)]
26. Xiao, W.-L.; Wu, Y.-L.; Shang, S.-Z.; He, F.; Luo, X.; Yang, G.-Y.; Pu, J.-X.; Chen, G.-Q.; Sun, H.-D. Four New Nortriterpenoids from *Schisandra lancifolia*. *Helvetica Chim. Acta* **2010**, *93*, 1975–1982. [[CrossRef](#)]
27. Shi, Y.-M.; Xiao, W.-L.; Pu, J.-X.; Sun, H.-D. Triterpenoids from the Schisandraceae family: An update. *Nat. Prod. Rep.* **2014**, *32*, 367–410. [[CrossRef](#)]
28. Qin, D.; Shen, W.Y.; Gao, T.C.; Zuo, S.H.; Song, H.C.; Xu, J.R.; Yu, B.H.; Peng, Y.J.; Guo, J.L.; Tang, W.W.; et al. Ka-danguslactones A-E, further oxygenated terpenoids from *Kadsura angustifolia* fermented by a symbiotic endophytic fungi, *Penicillium ochrochloron* SWUKD4.1850. *Phytochemistry* **2020**, *174*, 112335. [[CrossRef](#)]
29. Han, M.; Qin, D.; Ye, T.; Yan, X.; Wang, J.; Duan, X.; Dong, J. An endophytic fungus from *Trichoderma harzianum* SWUKD3.1610 that produces nigranoic acid and its analogues. *Nat. Prod. Res.* **2018**, *33*, 2079–2087. [[CrossRef](#)]
30. Huang, Q.; An, H.; Song, H.; Mao, H.; Shen, W.; Dong, J. Diversity and biotransformative potential of endophytic fungi associated with the medicinal plant *Kadsura angustifolia*. *Res. Microbiol.* **2014**, *166*, 45–55. [[CrossRef](#)]
31. Bai, Y.; Müller, D.B.; Srinivas, G.; Garrido-Oter, R.; Pothhoff, E.; Rott, M.; Dombrowski, N.; Münch, P.C.; Spaepen, S.; Remus-Emsermann, M.; et al. Functional overlap of the Arabidopsis leaf and root microbiota. *Nature* **2015**, *528*, 364–369. [[CrossRef](#)]
32. Thompson, J.D.; Higgins, D.; Gibson, T.J. CLUSTAL W: Improving the sensitivity of progressive multiple sequence alignment through sequence weighting, position-specific gap penalties and weight matrix choice. *Nucleic Acids Res.* **1994**, *22*, 4673–4680. [[CrossRef](#)]
33. Saitou, N.; Nei, M. The neighbor-joining method: A new method for reconstructing phylogenetic trees. *Mol. Biol. Evol.* **1987**, *4*, 406–425. [[CrossRef](#)]
34. Hussain, A.; Hasnain, S. Interactions of bacterial cytokinins and IAA in the rhizosphere may alter phytostimulatory efficiency of rhizobacteria. *World J. Microbiol. Biotechnol.* **2011**, *27*, 2645–2654. [[CrossRef](#)]
35. Alexander, D.B.; Zuberer, D.A. Use of chrome azurol S reagents to evaluate siderophore production by rhizosphere bacteria. *Biol. Fertil. Soils* **1991**, *12*, 39–45. [[CrossRef](#)]
36. Yokozawa, T.; Dong, E.; Nakagawa, T.; Kashiwagi, H.; Nakagawa, H.; Takeuchi, S.; Chung, H.Y. In Vitro and in Vivo Studies on the Radical-Scavenging Activity of Tea. *J. Agric. Food Chem.* **1998**, *46*, 2143–2150. [[CrossRef](#)]
37. Gyaneshwar, P.; Kumar, G.N.; Parekh, L.J.; Poole, P.S. Role of soil microorganisms in improving P nutrition of plants. *Plant. Soil* **2002**, *245*, 83–93. [[CrossRef](#)]
38. Moron-Rios, A.; Gómez-Cornelio, S.; Morales, B.O.O.; De la Rosa-García, S.; Partida-Martinez, L.P.; Quintana, P.; Alayón-Gamboa, J.A.; Cappello-García, S.; González-Gómez, S. Interactions between abundant fungal species influence the fungal community assemblage on limestone. *PLoS ONE* **2017**, *12*, e0188443. [[CrossRef](#)]
39. Niu, B.; Paulson, J.N.; Zheng, X.; Kolter, R. Simplified and representative bacterial community of maize roots. *Proc. Natl. Acad. Sci. USA* **2017**, *114*, E2450–E2459. [[CrossRef](#)] [[PubMed](#)]
40. Smith, R.H. *Plant Tissue Culture*, 3rd ed.; Academic Press: Cambridge, MA, USA, 2013; Chapter 12 In Vitro Propagation for Commercial Production of Ornamentals; pp. 127–145. [[CrossRef](#)]
41. Durán, P.; Thiergart, T.; Garrido-Oter, R.; Agler, M.; Kemen, E.; Schulze-Lefert, P.; Hacquard, S. Microbial Interkingdom Interactions in Roots Promote Arabidopsis Survival. *Cell* **2018**, *175*, 973–983. [[CrossRef](#)]
42. Tilahun, S.; An, H.S.; Solomon, T.; Baek, M.W.; Choi, H.R.; Lee, H.C.; Jeong, C.S. Indices for the Assessment of Glycoalkaloids in Potato Tubers Based on Surface Color and Chlorophyll Content. *Horticulturae* **2020**, *6*, 107. [[CrossRef](#)]
43. Kamonwannasit, S.; Nantapong, N.; Kumkrai, P.; Luecha, P.; Kupittayanant, S.; Chudapongse, N. Antibacterial activity of *Aquilaria crassna* leaf extract against *Staphylococcus epidermis* by disruption of cell wall. *Ann. Clin. Microbiol.* **2013**, *12*, 20. [[CrossRef](#)] [[PubMed](#)]
44. Boulet, J.-C.; Trarieux, C.; Souquet, J.-M.; Ducasse, M.-A.; Caillé, S.; Samson, A.; Williams, P.; Doco, T.; Cheynier, V. Models based on ultraviolet spectroscopy, polyphenols, oligosaccharides and polysaccharides for prediction of wine astringency. *Food Chem.* **2016**, *190*, 357–363. [[CrossRef](#)]
45. Sun, H.; Zhang, Z. Spectrophotometric methods to determine the grand total of the triterpenoids in *Betula*. *J. Nanjing For. Univ.* **2005**, *29*, 110–112. [[CrossRef](#)]
46. Lin, Y.; Lu, M.-F.; Liao, H.-B.; Li, Y.-X.; Han, W.; Yuan, K. Content determination of the flavonoids in the different parts and different species of *Abelmoschus esculentus* L. by reversed phase-high performance liquid chromatograph and colorimetric method. *Pharmacogn. Mag.* **2014**, *10*, 278–284. [[CrossRef](#)] [[PubMed](#)]
47. Singleton, V.L.; Rossi, J.A. Colorimetry of total phenolics with phosphomolybdic-phosphotungstic acid reagents. *Am. J. Enol. Viticult.* **1965**, *16*, 144–158.
48. Sun, H.-D.; Qiu, S.-X.; Lin, L.-Z.; Wang, Z.-Y.; Lin, Z.-W.; Pengsuparp, T.; Pezzuto, J.M.; Fong, H.H.S.; Cordell, G.A.; Farnsworth, N.R. Nigranoic Acid, a Triterpenoid from *Schisandra sphaerandra* That Inhibits HIV-1 Reverse Transcriptase. *J. Nat. Prod.* **1996**, *59*, 525–527. [[CrossRef](#)]

49. Dai, P.; Han, G.Q.; Arison, B.H. A new triterpenoid from *Kadsura heteroclita* (Roxb) Craib. *Chem. Res. Chin. Univ.* **1990**, *11*, 423–424.
50. Li, R.-T.; Han, Q.-B.; Zheng, Y.-T.; Wang, R.-R.; Yang, L.-M.; Lu, Y.; Sang, S.-Q.; Zheng, Q.-T.; Zhao, Q.-S.; Sun, H.-D. Structure and anti-HIV activity of micrandilactones B and C, new nortriterpenoids possessing a unique skeleton from *Schisandra micrantha*. *Chem. Commun.* **2005**, 2936–2938. [[CrossRef](#)]
51. Li, R.T.; Xiang, W.; Li, S.H.; Lin, Z.W.; Sun, H.D. Lancifodilactones B-E, New Nortriterpenes from *Schisandra lancifolia*. *J. Nat. Prod.* **2004**, *67*, 94–97. [[CrossRef](#)]
52. Szucs, Z.; Plaszkó, T.; Cziaky, Z.; Kiss-Szikszai, A.; Emri, T.; Bertoti, R.; Sinka, L.T.; Vasas, G.; Gonda, S. Endophytic fungi from the roots of horseradish (*Armoracia rusticana*) and their interactions with the defensive metabolites of the glucosinolate-myrosinase-isothiocyanate system. *BMC Plant Biol.* **2018**, *18*, 85. [[CrossRef](#)]
53. Tian, Y.; Amand, S.; Buisson, D.; Kunz, C.; Hachette, F.; Dupont, J.; Nay, B.; Prado, S. The fungal leaf endophyte *Paraconiothyrium variabile* specifically metabolizes the host-plant metabolome for its own benefit. *Phytochemistry* **2014**, *108*, 95–101. [[CrossRef](#)] [[PubMed](#)]
54. Haack, F.S.; Poehlein, A.; Kröger, C.; Voigt, C.; Piepenbring, M.; Bode, H.B.; Daniel, R.; Schäfer, W.; Streit, W.R. Molecular Keys to the Janthinobacterium and *Duganella* spp. Interaction with the Plant Pathogen *Fusarium graminearum*. *Front. Microbiol.* **2016**, *7*, 1668. [[CrossRef](#)] [[PubMed](#)]
55. Thakur, R.; Sharma, K.C.; Gulati, A.; Sud, R.K.; Gulati, A. Stress-Tolerant *Viridibacillus arenosi* Strain IHB B 7171 from Tea Rhizosphere as a Potential Broad-Spectrum Microbial Inoculant. *Indian J. Microbiol.* **2017**, *57*, 195–200. [[CrossRef](#)] [[PubMed](#)]
56. Wu, L.; Liu, R.; Niu, Y.; Lin, H.; Ye, W.; Guo, L.; Hu, X. Whole genome sequence of *Pantoea ananatis* R100, an antagonistic bacterium isolated from rice seed. *J. Biotechnol.* **2016**, *225*, 1–2. [[CrossRef](#)]
57. Sajitha, K.L.; Dev, S.A.; Florence, E.J.M. Biocontrol potential of *Bacillus subtilis* B1 against sapstain fungus in rubber wood. *Eur. J. Plant Pathol.* **2017**, *150*, 237–244. [[CrossRef](#)]
58. Naureen, Z.; Rehman, N.U.; Hussain, H.; Hussain, J.; Gilani, S.A.; Al Housni, S.K.; Mabood, F.; Khan, A.L.; Farooq, S.; Abbas, G.; et al. Exploring the Potentials of *Lysinibacillus sphaericus* ZA9 for Plant Growth Promotion and Biocontrol Activities against Phytopathogenic Fungi. *Front. Microbiol.* **2017**, *8*, 1477. [[CrossRef](#)]
59. Chopra, A.; Vandana, U.K.; Rahi, P.; Satpute, S.; Mazumder, P.B. Plant growth promoting potential of *Brevibacterium sediminis* A6 isolated from the tea rhizosphere of Assam, India. *Biocatal. Agric. Biotechnol.* **2020**, *27*, 101610. [[CrossRef](#)]
60. Mosquera-Espinosa, A.T.; Bayman, P.; Prado, G.A.; Gómez-Carabalí, A.; Otero, J.T. The double life of *Ceratobasidium*: Orchid mycorrhizal fungi and their potential for biocontrol of *Rhizoctonia solani* sheath blight of rice. *Mycologia* **2013**, *105*, 141–150. [[CrossRef](#)]
61. Zhang, Y.; Li, Y.; Chen, X.; Meng, Z.; Guo, S. Combined Metabolome and Transcriptome Analyses Reveal the Effects of Mycorrhizal Fungus *Ceratobasidium* sp. AR2 on the Flavonoid Accumulation in *Anoectochilus roxburghii* during Different Growth Stages. *Int. J. Mol. Sci.* **2020**, *21*, 564. [[CrossRef](#)]
62. Oztópuz, O.; Sarıgül, N.; Liaqat, F.; Park, R.-D.; Eltem, R. Chitinolytic *Bacillus subtilis* Ege-B-1.19 as a biocontrol agent against mycotoxicogenic and phytopathogenic fungi. *Turk. J. Biochem.* **2018**, *44*, 323–331. [[CrossRef](#)]
63. Kwak, M.-J.; Kong, H.G.; Choi, K.; Kwon, S.-K.; Song, J.Y.; Lee, J.; Lee, P.A.; Choi, S.Y.; Seo, M.; Lee, H.J.; et al. Correction: Author Correction: Rhizosphere microbiome structure alters to enable wilt resistance in tomato. *Nat. Biotechnol.* **2018**, *36*, 1117. [[CrossRef](#)] [[PubMed](#)]
64. Yan, L.; Khan, R.A.A. Biological control of bacterial wilt in tomato through the metabolites produced by the biocontrol fungus, *Trichoderma harzianum*. *Egypt. J. Biol. Pest. Control.* **2021**, *31*, 1–9. [[CrossRef](#)]
65. Wei, F.; Zhang, Y.; Shi, Y.; Feng, H.; Zhao, L.; Feng, Z.; Zhu, H. Evaluation of the Biocontrol Potential of Endophytic Fungus *Fusarium solani* CEF559 against *Verticillium dahliae* in Cotton Plant. *BioMed Res. Int.* **2019**, *2019*, 1–12. [[CrossRef](#)] [[PubMed](#)]
66. Han, Q.; Ma, Q.; Chen, Y.; Tian, B.; Xu, L.; Bai, Y.; Chen, W.; Li, X. Variation in rhizosphere microbial communities and its association with the symbiotic efficiency of rhizobia in soybean. *ISME J.* **2020**, *14*, 1915–1928. [[CrossRef](#)]
67. Gohil, N.; Bhattacharjee, G.; Singh, V. Synergistic bactericidal profiling of prodigiosin extracted from *Serratia marcescens* in combination with antibiotics against pathogenic bacteria. *Microb. Pathog.* **2020**, *149*, 104508. [[CrossRef](#)] [[PubMed](#)]
68. Aguilar-Pérez, M.M.; Torres-Mendoza, D.; Vásquez, R.; Rios, N.; Cubilla-Rios, L. Exploring the Antibacterial Activity of *Pestalotiopsis* spp. under Different Culture Conditions and Their Chemical Diversity Using LC–ESI–Q–TOF–MS. *J. Fungi* **2020**, *6*, 140. [[CrossRef](#)]